

Design and Experimental Results of Universal Electric Vehicle Charger Using DSP

Ali Saadon Al-Ogaili*, IshakAris, Mohammad Lutfi Othman, Norhafiz Azis, Dino Isa, Yap Hoon

Universiti Putra Malaysia, Malaysia

Abstract

Owing to the growing concerns over energy depletion and environmental issues around the world, more and more attention is given on replacing the fuel-based automobiles with electric vehicles (EVs) which have the characteristics of zero-emission and low noise. As a result, various countries have taken specific initiatives to de-carbonize their transport sectors by developing their own EV industry. Regardless of the environmental and economic benefits, substantial scales of grid-connected EVs impose incredible difficulties to the power grid. The main issues caused by EV charging to the power grid include harmonics, voltage drop, system instability, system losses and grid overloading. Therefore, this paper presents design and development of a novel method, which is by applying voltage-oriented control (VOC) algorithm in battery charging of electric bus. The power system of this work consists of three-phase PWM rectifier. The proposed method is based on mathematical analysis. Simulation and experimental works are performed to investigate behavior and performance of the proposed algorithm. This paper clearly described implementation of low and medium power laboratory prototype and operation of digital signal processor (DSP) via MATLAB / Simulink for the proposed method.

Keywords: Dq-theory; electric vehicle (EV); power factor; total harmonic distortion (THD); voltage-oriented control (VOC)

Copyright © 2018 Universitas Ahmad Dahlan. All rights reserved.

1. Introduction

ELECTRIC vehicles (EVs) are basically controlled by using an electric motor, which is usually powered up by a rechargeable battery. Presently, strong desire on implementing EVs with high performance quality has posted significant challenges and stresses on the capabilities of traditional battery systems. Unfortunately, as technology of battery advances, battery charging becomes exceptionally complicated due to involvement of high voltages and currents in the system. Hence, it requires complex charging techniques [1-3] to ensure effective and efficient charging. This further imposes great distortions in the operating ac power system and thus an efficient and low-distortion charger is highly needed.

Owing to the issues stated above, battery charging technology faces great deal of challenges. For instance, how to steadily and efficiently charge the battery, lengthen its operational life and so on, has tormented the researchers, designers and engineers all the time. The technology of battery varies differently. Nevertheless, the two commonly applied charging techniques are known as the constant-pressure and constant-current charging techniques. Basically, for battery charging, a tributary constant-current power supply (simply known as constant-current charger) is commonly adopted as external ac voltage which is supplied to the charger fluctuates continuously. Besides, by using the constant-current charging technique, the charging efficiency of the battery can be further increased. Moreover, the technique is also capable of deciding whether to conveniently terminate the charging process based on charging time and change the numbers of battery [4-7].

On the other hand, constant-pressure charging is another widely applied charging technique where the idea is to maintain a constant battery voltage between the poles. The main benefit is that it can automatically adjust the charging current according to the changes occurred in the battery state-of-charge. For instance, when the voltage has constantly been maintained at a suitable level, it is not only able to guarantee that the battery is fully charged, but it is also capable of minimizing the gas chromatography and desiccation. Moreover, various approaches are available for battery charging such as phase charging and float filling modes [8-13].

Based on the input supply of the national grid, this paper presents detailed modeling and design of a nearly optimum ac current and dc voltage controllers of the voltage-oriented controlled (VOC) grid connected rectifiers as shown in Figure 1. The design takes into consideration all practical aspects. Additionally, the effect of controller's parameters on the performance of the rectifier is also clearly described. Design concept and effectiveness of the VOC algorithm are confirmed through extensive simulations and experiments.

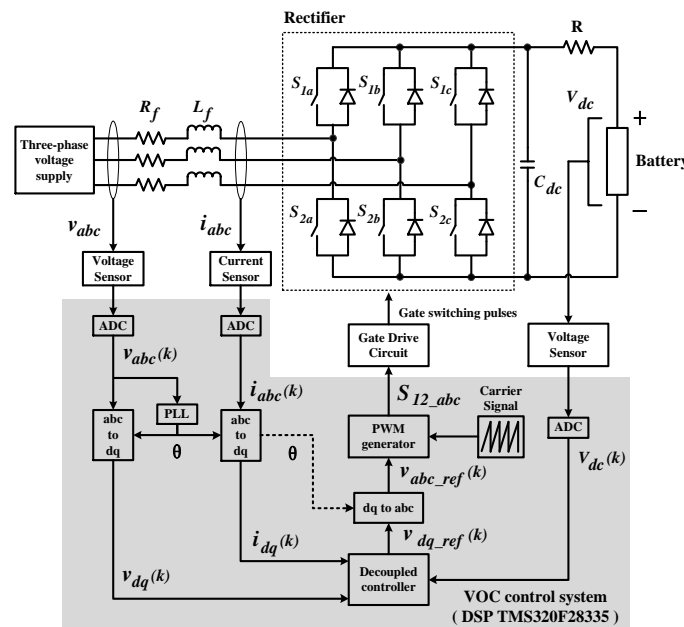


Figure 1. Three-phase PWM bridge rectifier of the proposed battery charger with VOC control algorithm

2. Modeling the System by Using Voltage-Oriented Control (VOC) Algorithm

Highly developed control techniques for grid-connected rectifiers apply the theory of decoupled active power and reactive power control which is performed in the synchronous reference direct-quadrature (dq) frame. By using this approach, which is also called the VOC, the required three-phase ac current is first transformed and decoupled into active (direct) i_d and reactive (quadrature) i_q component respectively.

The decoupled active and reactive components are then controlled in such a way that the errors between the desired reference and measured values of the active and reactive powers are removed. Generally, the active current component i_d is regulated by using a dc-link voltage control approach which aims to achieve active power flow balance in the system, and meanwhile the reactive component i_q , is regulated to zero level to ensure unity power factor operation. The VOC technique applied for grid-connected rectifiers has widely been reported in its theoretical aspects. In this paper, three proportional-integral (PI) controllers for controlling the current components i_d , i_q and dc-link voltage V_{dc} are presented.

3. Decoupled Controller of the First Stage Using Voltage-Oriented Control (VOC)

Presently, three types of controllers have been modeled which includes hysteresis, proportional-integral (PI) and predictive dead-beat controllers. Most of control techniques have been proposed, they have high performance, but they still show some obstacles not presenting the decoupling of the active and reactive current components (not allowing the independent control of the active and reactive power).

The modules can further be classified into stationary and synchronous dq reference frame implementations based on the theory of ac machine in rotating field. The controller of

PWM rectifier is a useful solution through the application of synchronous frame controller. In this paper, the controller of PWM rectifier has been modeled in the rotating dq reference frame as shown in Figure 2. This type of controller is called voltage-oriented control (VOC) and it has high performance as the synchronous frame controller can effectively reduce steady-state error and provides quick transient reaction by decoupling control.

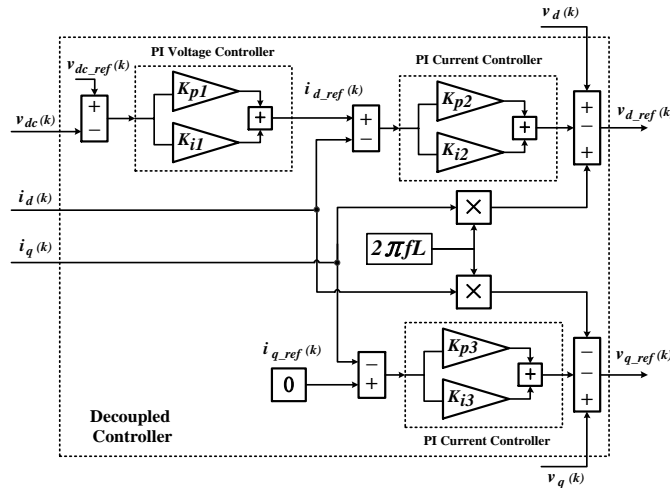


Figure 2. Decoupled controller

Based on Figure 3, the voltage equations based on Kirchhoff's voltage law (KVL) can be obtained. To mathematically derive the equation, we start from Figure 3 that shows three-phase PWM bridge rectifier connection to a grid. Based on Figure 3 v_a, v_b and v_c are the input voltages v_{in} of the grid and v_{ag}, v_{bg} and v_{cg} are the voltages of the rectifier side. The input filter implemented by simple L and R elements is the leakage reactance and resistance that connected between the grid and the rectifier. By applying KVL, the following relationship can be obtained:

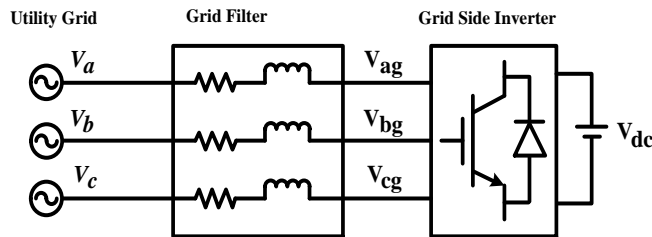


Figure 3. Modeling circuit of the grid-connected to the rectifier

$$v_{in} = i_{in}R + L \frac{di_{in}}{dt} + v_{in,g} \tag{1}$$

$$v_a = i_aR + L \frac{di_a}{dt} + v_{a,g} \tag{2}$$

$$v_b = i_bR + L \frac{di_b}{dt} + v_{b,g} \tag{3}$$

$$v_c = i_c R + L \frac{di_c}{dt} + v_{cg} \tag{4}$$

Next, by applying the theory of Park transformation as shown in Figure 4, voltages and currents can be transformed from abc system to dq frame as shown in Figure 5.

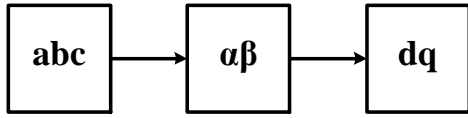


Figure 4. Park transformation

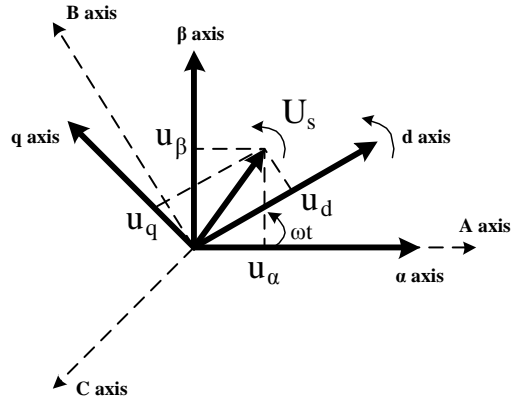


Figure 5. Phasor diagram of Park transformation

$$\begin{bmatrix} v_\alpha \\ v_\beta \\ v_0 \end{bmatrix} = \sqrt{\frac{2}{3}} \begin{bmatrix} 1 & -1 & -1 \\ 0 & \sqrt{3} & -\sqrt{3} \\ \frac{1}{\sqrt{2}} & \frac{1}{\sqrt{2}} & \frac{1}{\sqrt{2}} \end{bmatrix} \begin{bmatrix} v_a \\ v_b \\ v_c \end{bmatrix} \tag{5}$$

$$\begin{bmatrix} v_d \\ v_q \\ v_0 \end{bmatrix} = \begin{bmatrix} \cos \theta & \sin \theta & 0 \\ -\sin \theta & \cos \theta & 0 \\ 0 & 0 & 1 \end{bmatrix} \begin{bmatrix} v_\alpha \\ v_\beta \\ v_0 \end{bmatrix} \tag{6}$$

where v indicates voltage. Hence, by applying the Park transformation in the stationary reference frame to (1), the following relation holds

$$\vec{v}_{in\alpha\beta} - v_{g\alpha\beta} = L \frac{d}{dt} \vec{i}_{\alpha\beta} + R \vec{i}_{\alpha\beta} \tag{7}$$

By considering $\vec{x}_{\alpha\beta} = \vec{x}_{dq} e^{j\omega t}$, (7) can be rewritten as (8)

$$\vec{v}_{indq} - v_{gdq} = L \frac{d}{dt} \vec{i}_{dq} + (R + jL\omega) \vec{i}_{dq} \tag{8}$$

The voltage equations in dq synchronous reference frame are given by:

$$v_d = i_{dg} R_g + L_g \frac{di_{dg}}{dt} - 2\pi f L_g i_{qg} + v_{dg} \tag{9}$$

$$v_q = i_{qg} R_g + L_g \frac{di_{qg}}{dt} + 2\pi f L_g i_{dg} + v_{qg} \tag{10}$$

The power balance equations are:

$$P = \frac{3}{2} Re\{v^{dq}(i^{dq})^*\} = \frac{3}{2}(v_d i_d + v_q i_q) = \frac{3}{2}(E_d i_d + E_q i_q) \tag{11}$$

$$Q = \frac{3}{2} Im\{v^{dq}(i^{dq})^*\} = \frac{3}{2}(v_q i_d - v_d i_q) = \frac{3}{2}(E_q i_d - E_d i_q) \tag{12}$$

where P is active power and Q is reactive power. Since the d-axis rotating reference is aligned with grid voltage vector, hence E_q can be set at zero and q-axis current is set at zero under normal conditions to maintain unity power factor (PF) at grid side converter. With this the power balance equation becomes:

$$P = \frac{3}{2} E_d i_d \tag{13}$$

$$Q = 0 \tag{14}$$

This decoupling makes active and reactive power to control independently by controlling the d-axis and q-axis currents as shown in Figure 6.

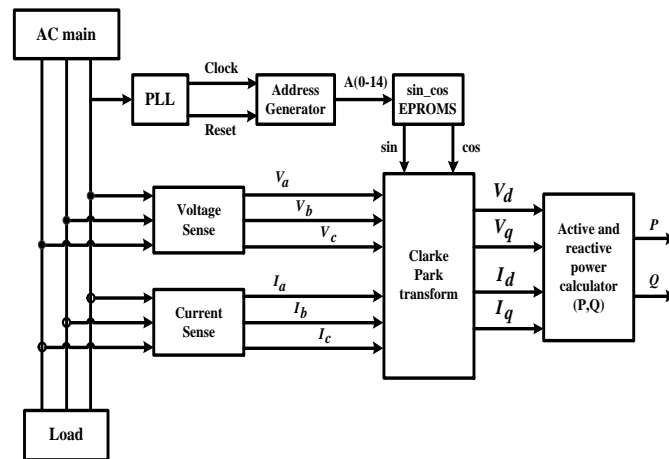


Figure 6. Circuit configuration of the active power P and reactive power Q based on Clarke and Park transform.

4. Simulation Results

The proposed rectifier system with VOC control algorithm as shown previously in Figure 1 is simulated and evaluated in MATLAB/Simulink. All the design and test parameters applied for the simulation work is summarized in Table 1.

Table 1. Parameters for Simulation and Experimental Work

Parameter	Value
Resistor load R_{load}	250 Ω
Input inductance filter L_f	5 mH
Dc-link capacitor C	2200 μ F
Dc-link reference voltage $V_{dc.ref}$	100 V
Supply voltage frequency f	50 Hz
Switching frequency f_s	12 kHz
Input resistance filter R_f	1 Ω

Figure 7 shows a sinusoidal reference voltages $v_{(a_ref)}$ which is used to generate PWM switching pulses based on intersections with triangular carrier signal. The idea is to directly

compare the three sinusoidal reference voltages $v_{(a_ref)}$, $v_{(b_ref)}$ and $v_{(c_ref)}$ with the triangular carrier signal. As a result of the comparative process, the desired switching pulses S_{1abc} and S_{2abc} for controlling the operation of each power transistor of the rectifier, are generated.

By accurately control the reference voltage and maintaining its peak value at constant value of 1V, the magnitude of the generated modulating signal will continuously be maintained at a level which is lower than the peak of the triangle carrier signal. In other words, the modulation process will always be maintained at linear modulation zone. This is crucial for ensuring proper generation of switching pulses. At any instance if the modulating signal is greater than the carrier signal, the upper switch of the rectifier will be turned "on" and the lower switch is "off". In contrast, if the modulating signal is less than the carrier signal, the upper switch will be turned "off" and the lower switch is "on". This shows that the operation of upper and lower switches of the rectifier is always complementing to each other.

Figure 8 shows the input voltage of phase A (110 V) and meanwhile Figure 9 shows the regulated output dc-link voltage. It is clear from Figures 8 and 9 that by using 110 V as input, the proposed control algorithm has accurately regulated and maintained the output dc-link voltage at desired level of 100 V. At the same time, by referring to Figure 10, it can be observed that a sinusoidal input current of phase A with minimum switching noises and total harmonic distortion (THD=3.36%) and a unity power factor ($i_q=0$) is produced. Finally, Figure 11 shows the output dc current with 0.01 ripples, this value of ripples do not cause any harms to the battery in case of charging a battery of electric bus. Therefore, it is clear that the proposed control algorithm performs effectively in providing a constant output voltage and current for battery charging with minimal disturbance to the operating power system.

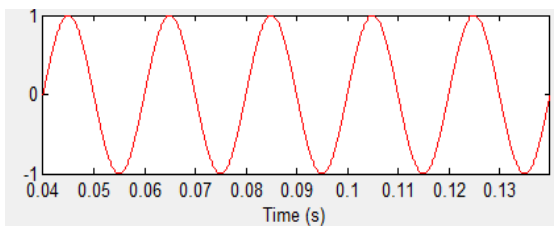


Figure 1. Reference voltage of phase A.

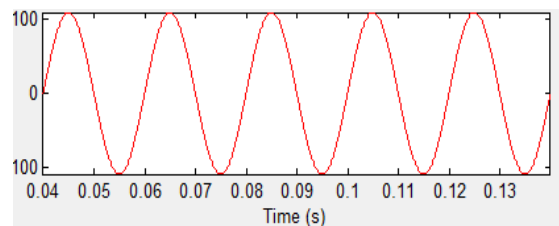


Figure 2. Input voltage ($V_{in} = 110$ V) of phase A.

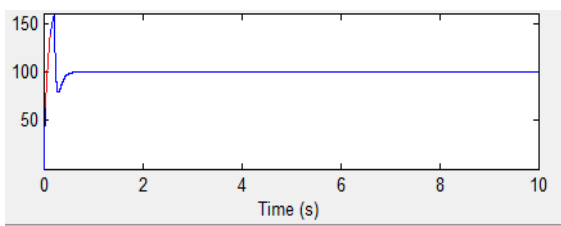


Figure 3. Output dc-link voltage with reference voltage ($V_{dc_ref} = 100$ V).

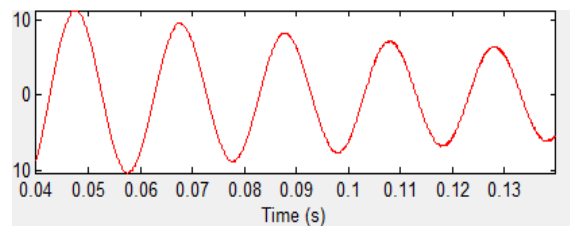


Figure 4. Input current of phase A.

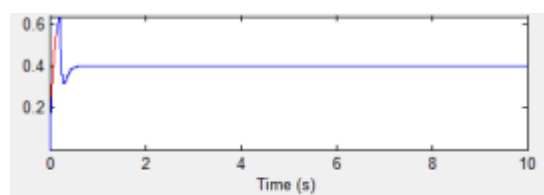


Figure 5. Output dc current ($V_{dc_ref} = 100$ V, $R_{load} = 250\Omega$).

Figure 12 and Figure 13 show the simulation result of the input voltage and current of the proposed circuit which can fulfill the requirements of third level charging for Electric Bus/Lorry (fast charging).. The physical aspect of these results show almost pure sinusoidal waveform of the input voltage and the THD for the input current is recorded at 4.11 %. Next, Figure 14 demonstrates how the proposed control system can effectively present an accurate regulation of dc-link voltage at the dc reference voltage of 650 V. By using three-phase input supply voltage of 700 V and resistive load of 250 Ω, regulated dc voltage as shown in Figure 14 (a) and dc current as shown in Figure 14 (b)

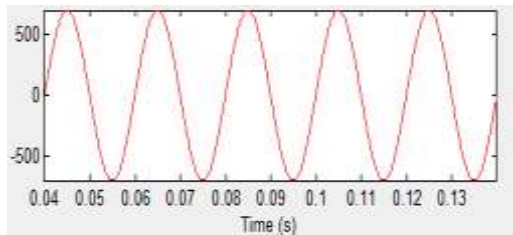


Figure 6. Input voltage (700V) of phase A

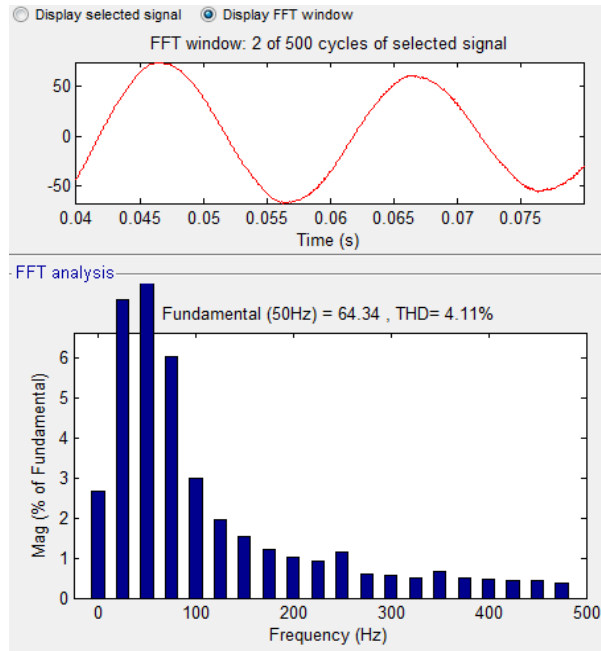


Figure 7. Input current of phase A.

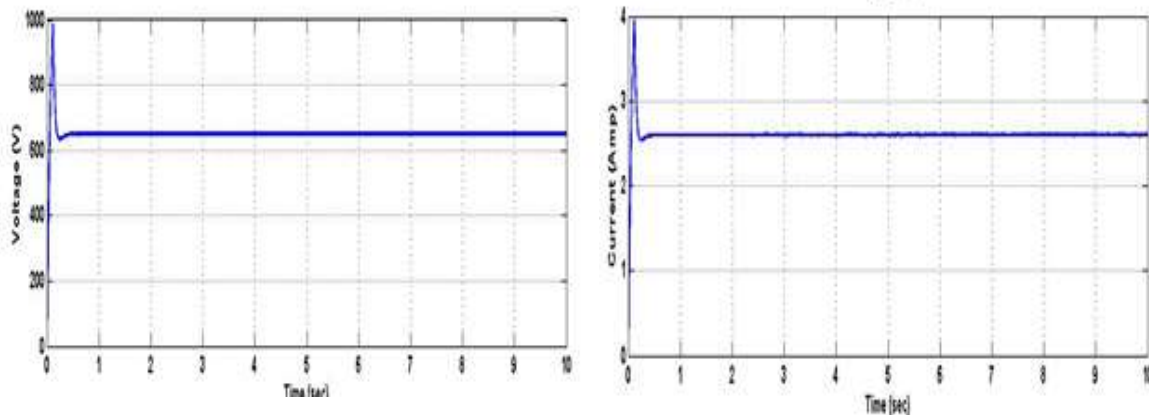


Figure 8. The dcoutput of VOC: (a) regulated voltage and (b) current respectively.

5. Experimental Results

Laboratory prototype is developed to validate practically effectiveness of the proposed VOC algorithm. Experimental setup for the proposed rectifier with VOC algorithm is shown in Figure 15. Meanwhile, Figure 16 shows the VOC algorithm which is downloaded into a TMS320F28335 digital signal processor (DSP) from TexasInstruments (TI). The design and

test parameters applied for experiment work is similar to the one applied in simulation work, as summarized in Table 1.

The performance demonstrated by the proposed control algorithm in response to step changes of dc voltage reference is shown in Figures 17 and 18. According to these figures, the ac current is working in the same phase with the ac voltage. Besides, it achieves almost unity power factor rectifier and thus fulfilling the requirements of the battery charger. Meanwhile, the output voltage and current are constant, and thus the battery charging of electric vehicle (EV) is stable.

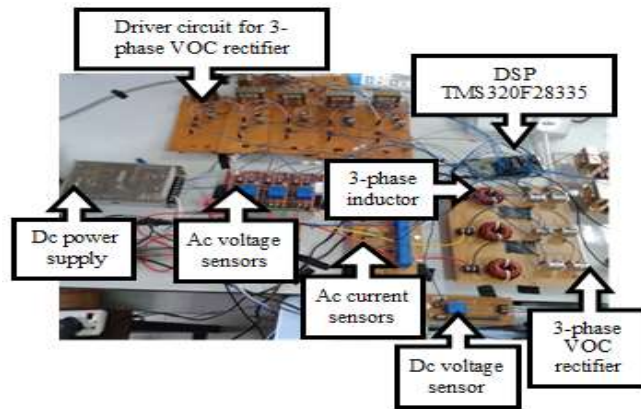


Figure 9. Experimental setup for rectifier with VOC control

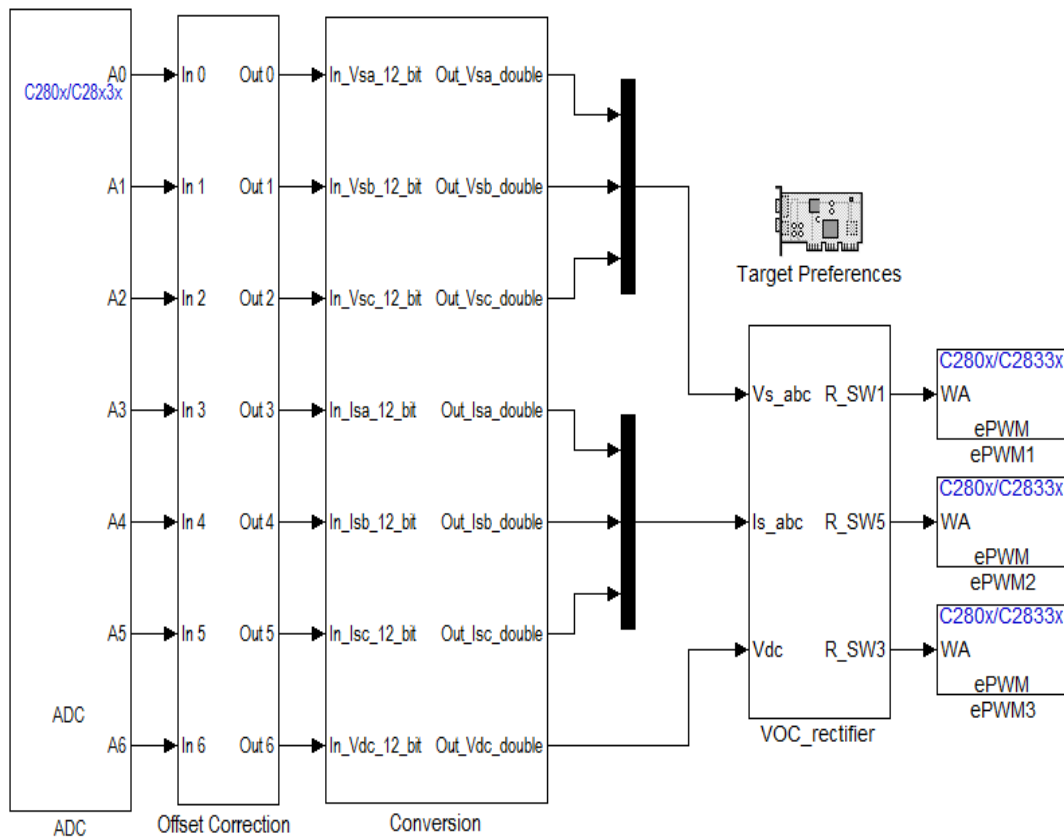


Figure 10. VOC control algorithm for DSP implementation

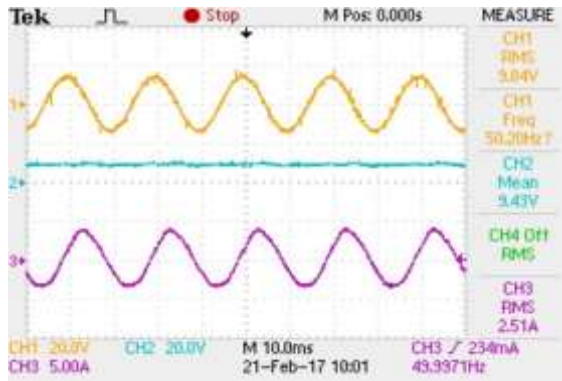


Figure 17. Input voltage of phase A(CH1), output dc voltage (CH2) and input current of phase A (CH3)

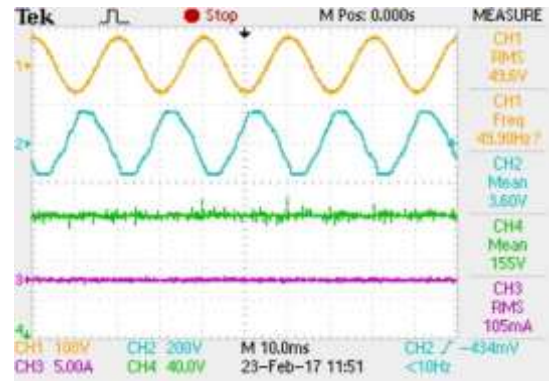


Figure 18. Reference voltage of phase A (CH1), input voltage of phase A (CH2), output dc-link voltage (CH4) and output dc voltage (CH3)

6. Conclusion

This paper has clearly demonstrated a VOC control algorithm for effective operation of three-phase PWM rectifier in generating constant output dc voltage and current. From the findings, it is clear that the control algorithm accurately regulates the dc-link voltage at desired level and at the same time, it ensures sinusoidal input current with minimum switching ripples and distortions, where THD of the input current is maintained at 4.11 % with an almost unity power factor.

7. Highlights:

- This paper addresses the design and development of vehicle (EV) charger which is appropriate Level 3 charging.
- VOC control algorithm and SPWM switching algorithm are applied to effectively control the charging process. The algorithms are successfully implemented digitally on TMS320F28335 digital signal processor (DSP) board.
- The simulation and experimental results demonstrated effectiveness of the proposed algorithms in providing constant DC output voltage and current for stable and secure battery charging.
- The power factor of the input is almost unity, and the total harmonic distortion (THD) for the input current is less than 5 %. The overall efficiency based on simulation results is more than 97%.

References

- [1] Texas Instruments. Hybrid and Electric Vehicle Solutions Guide. <http://www.ti.com/lit/ml/szza058a/szza058a.pdf>.
- [2] K. T. Chau and Y. S. Wong. Overview of power management in hybrid electric vehicles. *Energy Conversion and Management*. 2002; 43(15):1953-1968.
- [3] Pesaran. *Battery Requirements for Plug-In Hybrid Electric Vehicles – Analysis and Rational*. presented in Sustainability: The Future of Transportation, EVS, Dec. 2007.
- [4] W. Chen, X. Ruan, and R. Zhang. A novel zero-voltage switching PWM full bridge converter. *IEEE Trans. Power Electron.* 2008; 23(2):793–801.
- [5] A. J. Mason, D. J. Tschirhart, and P. K. Jain. New ZVS phase shift modulated full-bridge converter topologies with adaptive energy storage for SOFC application. *IEEE Trans. Power Electron.* 2008; 23(1); 332–342.
- [6] M. Borage, S. Tiwari, S. Bhardwaj, and S. Kotaiah. A full bridge DC–DC converter with zero-voltage-switching over the entire conversion range. *IEEE Trans. Power Electron.* 2008; 23(4):1743–1750.
- [7] B.-Y. Chen and Y.-S. Lai. Switching control technique of phase-shift controlled full-bridge converter to improve efficiency under light-load and standby conditions without additional auxiliary components. *IEEE Trans. Power Electron.* 2010; 25(4):1001–1012.

-
- [8] W. Chen, X.Ruan, Q. Chen, and J. Ge. Zero-voltage switching PWM full bridge converter employing auxiliary transformer to reset the clamping diode current. *IEEE Trans. Power Electron.* 2010; 25 (5):1149–1162.
 - [9] M. Ordonez and J. E. Quaiçoe. Soft-switching techniques for efficiency gains in full-bridge fuel cell power conversion. *IEEE Trans. Power Electron.* 2011; 26 (2): 482–492.
 - [10] Shen IM, Jou HL, Wub JC, Wua KD. Single-phase three-wire grid-connected power converter with energy storage for positive grounding photovoltaic generation system. *Int. J. Electr. Power Energy Syst.* 2014;54:134–43.
 - [11] Ninad NA, Lopes L. Per-phase vector control strategy for a four-leg voltage source inverter operating with highly unbalanced loads in stand-alone hybrid systems. *Int. J. Electr. Power Energy Syst.* 2014;55:449–59.
 - [12] Colak I, Kabalci. Developing a novel sinusoidal pulse width modulation (SPWM) technique to eliminate side band harmonics. *Int. J. Electr. Power Energy Syst.* 2013;44:861–71.
 - [13] Monfared M, Rastegar H. Design and experimental verification of a dead beat power control strategy for low cost three phase PWM converters. *Int. J. Electr. Power Energy Syst.* 2012;42:418–25.
 - [14] Bhat AH, Langer N. Supply perturbation compensated control scheme for three-phase neutral-point clamped bi-directional rectifier. *Int. J. Electr. Power Energy Syst.* 2014;54:17–25.